Title

Simultaneous optimization of RBE-weighted dose and nanometric ionization distributions in treatment planning with carbon ions

Journal

Physics in Medicine and Biology, 64(1)

ISSN

0031-9155

Authors

Burigo, Lucas N
Ramos-Méndez, José
Bangert, Mark
et al.

Publication Date

2019

DOI

10.1088/1361-6560/aaf400

Peer reviewed

Published in final edited form as:

Phys Med Biol. ; 64(1): 015015. doi:10.1088/1361-6560/aaf400.

Simultaneous optimization of RBE-weighted dose and nanometric ionization distributions in treatment planning with carbon ions

Lucas N Burigo[(1),(2)], **José Ramos-Méndez**[(3)], **Mark Bangert**[(1),(2)], **Reinhard W Schulte**[(4),(3)], **Bruce Faddegon**[(3)]

[(1)]German Cancer Research Center – DKFZ, Im Neuenheimer Feld 280, D-69120 Heidelberg, Germany

[(2)]Heidelberg Institute for Radiation Oncology – HIRO, Im Neuenheimer Feld 280, D-69120 Heidelberg, Germany

[(3)]University of California San Francisco Helen Diller Family Comprehensive Cancer Center, 1600 Divisadero Street, San Francisco, CA 94143-1708, USA

[(4)]Division of Biomedical Engineering Sciences, Loma Linda University, Loma Linda, CA 92350, USA

Abstract

Inverse treatment planning in intensity modulated particle therapy (IMPT) with scanned carbon-ion beams is currently based on the optimization of RBE-weighted dose to satisfy requirements of target coverage and limited toxicity to organs-at-risk and healthy tissues. There are many feasible IMPT plans that meet these requirements, which allows the introduction of further criteria to narrow the selection of a biologically optimal treatment plan. We propose a novel treatment planning strategy based on the simultaneous optimization of RBE-weighted dose and nanometric ionization details (ID) as a new physical characteristic of the delivered plan beyond LET. In particular, we focus on the distribution of large ionization clusters (more than 3 ionizations) to enhance the biological effect across the target volume while minimizing biological effect in normal tissues. Carbon-ion treatment plans for different patient geometries and beam configurations generated with the simultaneous optimization strategy were compared against reference plans obtained with RBE-weighted dose optimization alone. Quality indicators, inhomogeneity index and planning volume histograms of RBE-weighted dose and large ionization clusters were used to evaluate the treatment plans. We show that with simultaneous optimization, ID distributions can be optimized in carbon-ion radiotherapy without compromising the RBE-weighted dose distributions. This strategy can potentially be used to account for optimization of endpoints closely related to radiation quality to achieve better tumor control and reduce risks of complications.

Keywords

biological optimization; treatment planning; IMPT; carbon ion; nanodosimetry; LET

1 Introduction

State-of-the-art treatment planning for scanned proton and carbon-ion radiotherapy requires the optimization of the fluence of discrete pencil beams, potentially delivered by several fields, to give a specific dose to the tumor while limiting the dose to surrounding tissue. This inverse planning process leads to the creation of intensity-modulated particle therapy (IMPT) plans. The biological optimization of IMPT treatment plans, in practice, is based on dose weighted by the relative biological effectiveness (RBE), optimized to be reasonably uniform throughout the target volume, and with dose constraints to organs-at-risk (OARs) (Krämer and Scholz 2000, Jäkel et al 2001). As the radiation effect induced by protons is similar to the one induced by photons, a common practice is to apply a constant RBE of 1.1 in the computation of RBE-weighted proton dose. However, the use of a constant RBE for protons has been questioned, mainly because of the observed increase in RBE at the distal edge of the depth-dose curve (Paganetti 2014). Conversely, the radiation effect induced by carbon ions and other heavy ions is strikingly different than for photons or protons for the same absorbed dose, showing a rather complex dependence on several physical, biological, and clinical quantities (e.g., ion type and energy, dose, cell type, biological or clinical endpoint etc.). Such dependencies are accounted for in IMPT plans by means of radiobiological modeling of the radiation effect on tumor and normal tissues.

Different models have been proposed to account for the complex dependencies of RBE on many factors, albeit with relatively large uncertainties in RBE. The Local Effect Model (LEM) (Scholz and Kraft 1996, Scholz et al 1997, Elsässer and Scholz 2007) is clinically used for this purpose at the European carbon-ion centers, while the Microdosimetric Kinetic Model (MKM) (Hawkins 2003, Inaniwa et al 2010) has been adopted at the Heavy Ion Medical Accelerator in Chiba, Japan. Despite the relative success of this strategy, allowing patients to be treated with carbon ions at acceptable risk for late effects, different approaches have been suggested in order to incorporate additional physical aspects of the radiation quality in the treatment planning optimization, which are not necessarily accounted for in the RBE modeling and may further improve clinical results. The main rationale is that the optimization of physical quantities has a potential to reduce the uncertainties connected to RBE.

For hypoxic tumors, Bassler and co-authors have considered the so-called LET-painting approach (Bassler et al 2010, Bassler *et al* 2014), concluding that without disturbing the physical dose it is possible to achieve an additional therapeutic advantage when high-LET radiation is confined to hypoxic subvolumes of the tumor, while the normoxic tumor is primarily irradiated by low-LET radiation. Tinganelli et al (2015) investigated the case of tumors presenting a variable radiosensitivity due to in-homogeneous oxygen concentration. Their so-called kill-painting approach intrinsically accounts for the voxel-based LET distribution inside the target when optimizing the fluence of the individual beam spots in the treatment plan in order to achieve uniform response across the target volume.

A potential clinical benefit was sought by minimization of LET in the OAR as reported by Giantsoudi *et al* who considered a multicriteria optimization strategy for proton IMPT using dose and LET distributions for guidance (Giantsoudi et al 2013). The authors suggested the

use of a hybrid optimization approach with objectives based on dose and LET to investigate whether the observed trade-off of low dose and low LET in the Pareto-surface navigation would hold. In the same way, a prioritized optimization approach for IMPT plans in proton therapy was suggested by Unkelbach and colleagues to avoid elevated LET in serial-type critical structures overlaying the target volume (Unkelbach et al 2016) for patients with intracranial tumors, e.g., optic nerves and brain stem. They concluded that this approach could provide safer IMPT treatments by reducing the potential increased risk of side effects resulting from high LET at the end of the proton range.

Recently, a new therapeutic technique comprising the combination of different ion species for treatment, namely, protons, helium, carbon and oxygen ions, to take advantage of the variation of LET as a function of ion type was investigated by Inaniwa et al (2017). Using simultaneous optimization of physical dose and dose-averaged LET in the patient, they could obtain uniform physical dose and LET distributions in the target volume by appropriate weighting of the ion species. A range of LET values depending on target size and beam configuration could be achieved, suggesting that their strategy could help to maximize the potential of radiotherapy with ion beams as it provides a means to expand the therapeutic window.

Simultaneous optimization of physical dose and dose-averaged LET was also considered by Cao et al 2018 for IMPT plans of brain tumors patients in proton therapy. The authors showed that a reduction of the dose-averaged LET at critical organs and increased LET in target volume could be achieved for comparable dose distributions obtained through conventional dose-based optimization alone.

While the aforementioned studies have considered LET as a surrogate for radiation quality, it is known that LET alone presents limitations in the modeling of RBE as it only accounts for an average description of the stochastic energy deposition events on the scale of cells and DNA molecules. To overcome these limitations, microdosimetry and nanodosimetry techniques have been suggested (Rossi and Zaider 1991, Lindborg and Nikjoo 2011, Rabus and Nettelbeck 2011, Conte et al 2017) as more appropriate to quantify radiation effects, especially for high-LET radiation. Nanodosimetry makes an attempt to correlates the stochastic number of ionizations created by the passage of particles to the biological effectiveness of ionization radiation. Experiments have been developed to measure the distributions of ionization cluster size which corresponds to the number of ionizations created in a target volume comparable to a DNA segment. In particular, it has been suggested that ionization clustering could be applied as a surrogate of clustered DNA damage (Grosswendt et al 2007, Garty et al 2010). Along the same lines, Casiraghi and Schulte (2015) suggested an alternative approach for treatment planning, which relies only on nanodosimetry instead of the common practice of optimization of RBE-weighted dose. They proposed an optimization of the beam fluence to attain a uniform distribution of specific nanodosimetric quantities in the target volume, thus providing an RBE-independent approach to treatment plan optimization.

Since different IMPT plans can satisfy the conventional requirements on target coverage and sparing of healthy tissues, while differing with respect to the spatial and spectral distribution

of particles in the radiation field, a simultaneous optimization of RBE-weighted dose and other identifiers of radiation quality is possible. Simultaneous optimization of RBE-weighted dose using an RBE model in clinical use and an identifier of radiation quality such as ionization detail (ID) on the nanometer scale, or nanometric ionization details, may lead to new insights and eventually better outcomes. We propose a novel treatment planning approach based on simultaneous optimization of RBE-weighted dose and ID in the target volume and OARs. ID, as defined in Ramos-Méndez *et al*, refers to parameters used to quantify a detail of ionization distributions, including ionization cluster size and moments of the ionization cluster distribution. Different from the strategies presented above, ID is used in the present study as a quantitative measure of radiation quality instead of LET. A specific ID is chosen to represent nanometric ionization clustering for demonstration purposes. To our knowledge, this is the first study that presents a simultaneous optimization strategy of RBE-weighted dose and nanometric ionization clustering (ionization cluster size distributions on the nanometer scale) for IMPT treatment planning. The goal is to provide the means to incorporate ID into the treatment planning process to improve the therapeutic ratio while not interfering with the current clinical practice. The extent to which the approach impacts robustness was left for future studies.

2 Materials and methods

2.1 Treatment planning system

The research treatment planning system (TPS) matRad (Wieser et al 2017), developed at the Division of Medical Physics in Radiation Oncology in the German Cancer Research Center (DKFZ), was used for the generation of IMPT plans for carbon ion therapy. The TPS relies on generic base data for carbon ions to compute using the analytical pencil beam algorithm a dose influence matrix for each pencil beam spot composing the irradiation field. The dose influence matrix is then applied during inverse treatment planning optimization. A detailed description is given below.

2.1.1 Base data of carbon ions—The base data contains the necessary information to model the spatial distribution of dose and radiation quality in the patient of every single pencil beam. It was generated with the Monte Carlo method using TOPAS version 3.1 (Perl et al 2012) based on Geant4 toolkit version 10.3 patch 01 (Agostinelli et al 2003, Allison et al 2006). Laterally integrated base data of carbon-ion pencil beams was generated in water with the range varying from 30 to 300 mm in steps of 3 mm. A 3 mm ripple filter was simulated to broaden the peak width of the Bragg curve. The base data includes data on depth distributions of dose, LET, nanodosimetric quantities (e.g., moments of the ionization cluster size distribution) as well as alpha and beta parameters for different tissue radiosensitivities computed using the local effect concept of LEM I (Scholz et al 1997). The lateral dose profile was parametrized using a double Gaussian fit similar to the procedure described in Parodi et al (2013). For the current study, we used ID as a surrogate for radiation quality as this is believed to be more closely correlated with biological effect than LET. In particular, we computed the frequency distributions of clusters of ionizations produced in water cylinders of 10 base pairs length (3.4 nm distance) and 2.3 nm diameter irradiated by protons and heavier ions up to oxygen using Monte Carlo track structure

simulations (Ramos-Méndez *et al).* Such sensitive volume is typically used in nanodosimetry to relate ionization cluster size to DNA damage complexity (Grosswendt et al 2007). Ionization cluster sizes of 1 or 2 will rarely cause double strand breaks and are thus considered not biologically relevant. Cluster sizes 3 and larger, on the other hand, will be responsible for most DNA double strand breaks and also for less frequent bur more consequential complex DNA damages. Since we are interested in a nanodosimetric quantity that could be related to complex DNA damages, we arbitrarily neglected the ionization clusters smaller than 3 in our study. From the frequency distributions of clusters of ionizations, the absolute number of large ionization clusters per unit length, defined here as clusters consisting of 4 or more ionizations, was parametrized as a function of atomic number and kinetic energy and then applied in the calculation of ID-depth profiles for carbon-ion pencil beams in water. Further details on the procedure adopted for the calculation of ionization clusters is presented by Ramos-Méndez *et al.* Because the absolute number of large ionization clusters is an additive quantity, the distribution for an IMPT plan is obtained by summing up the absolute number of large ionization clusters produced by each individual pencil beam. In the case of LET distributions, dose-average LET at each voxel is computed by the sum of LET of each pencil beam weighted by its relative dose at the voxel (Granville D A, Sawakuchi G O, 2015).

2.1.2 Optimization procedure—IMPT plan optimization in matRad relies on the definition of a set of objective functions and constraints on the dose for segmented structures such as target volumes and OARs. For carbon ions, a biological dose optimization is performed where the objectives and constraints are calculated on the basis of RBE-weighted dose. The optimizer will then search for the corresponding fluence of each pencil beam spot in all the fields that minimizes the global objective function while satisfying the constraints. A detailed explanation of the optimization approach in matRad has been presented elsewhere (Wieser et al 2017).

While the original optimization approach in matRad allows the definition of multiple objectives and constraints for the optimization, such criteria have been based on (RBE-weighted) dose only. For the present investigation, the global objective function was extended to allow the combination of objectives on RBE-weighted dose and objectives on large ionization clusters ν_L comprising a hybrid global objective function applied in the minimization problem:

$$min\left[\chi(\vec{w}) = \sum_{i \in VOIs} p_{d,i} f_{d,i}(\vec{w}) + p_{\upsilon_L,i} f_{\upsilon_L,i}(\vec{w})\right]$$

where $f_{d,i}$ ($f_{\nu L,i}$) and $p_{d,i}$ ($p_{\nu L,i}$) denote the objective function and penalty for RBE-weighted dose (large ionization clusters) in the *i-th* volume of interest (VOI), respectively. The optimization of RBE-weighted dose in the target volume is obtained by the objective squared deviation which computes the cost as the sum of the squared difference between the dose in the voxel and the prescribed dose. As for the organs-at-risk, the objective squared overdosing computes the cost by the sum of the squared difference between the reference dose and the dose in the voxel for the voxels with dose above the reference value. Further

details on objective functions and penalties in matRad can be found in (Wieser et al 2017). Similarly, objective functions for the large ionization clusters are used to compute the cost associated with the changes in the number of large ionization clusters. In this way, when searching for the individual pencil beam fluences $\vec{w}$ that minimize the hybrid global objective function $\chi(\vec{w})$, the optimizer will simultaneously account for the objectives on different quantities subject to their respective constraints, simultaneously optimizing RBE-weighted dose and large ionization clusters.

In this work, a new objective function was defined in matRad for the investigation of simultaneous optimization of RBE-weighted dose and ID, namely an objective to minimize the normalized variance of the number of large ionization clusters in structure S,

$$f_{minimize\sigma^2 / \mu^2(v_L)} = \frac{N_S \sum_{j \in S} v_{L_j}^2}{\left(\sum_{j \in S} v_{L_j}\right)^2} - 1,$$

used to increase homogeneity in the distribution of large ionization clusters in the VOI. In addition, objectives analogous to square underdosing (square overdosing) were implemented to enhance (decrease) the number of large clusters in the VOI by penalizing values below (above) a reference value taken from the plan without simultaneous optimization.

The assignment of penalties for the objective functions and constraints of each VOI can have a critical impact on the results of the optimization. A higher penalty for a given planning objective will increase its relative cost and therefore set a higher priority in the optimization process what can hinder the optimization of the remaining objectives. Therefore, the penalty of objectives on large ionization clusters should be appropriately chosen to not undermine the optimization of dose objectives and constraints when applying the simultaneous optimization approach.

2.1.3 Validation—The accuracy of the matRad TPS with respect to the calculation of IMPT plans for carbon ions using the beam models commissioned for radiotherapy at Heildelberg Ion-Beam Therapy Center has been demonstrate elsewhere (Wieser et al 2017). For this study, we used a realistic generic beam model for the purpose of dose calculation with TOPAS, as the details required to model the clinical beams were not available. The accuracy of dose and ID calculation is not affected by the beam details, although the result cannot be reliably confirmed with measurement, since the beams are not available clinically.

In order to validate the simultaneous optimization approach, treatment plans obtained with the simultaneous optimization with matRad were recalculated using Monte Carlo simulations with TOPAS. A threshold of 0.5 mm for the production of secondary electrons was used and the total number of histories simulated was chosen in order to achieve a statistical uncertainty lower than 1% at the target volumes. The distributions of physical dose, RBE-weighted dose and large ionization clusters were compared against the results from matRad using the three-dimensional γ-analysis (Low et al 1998). A distance to agreement (dta) of 2 mm and a dose difference (Δd) criterion of 2% was applied. In order to

evaluate the distribution of large ionization clusters, a difference criterion of 2% on the number of large clusters was considered.

2.2 Patient selection and definition of treatment plans

In order to evaluate the potential of simultaneous optimization for different endpoints under varying irradiation conditions, we investigated four treatment plans for different phantom and patient geometries. The selected geometries were: i) a simplified homogeneous cubic water phantom with a centered cubic planned target tumor (PTV) and an insert in the PTV representing a radioresistant subvolume (case 1) or ii) a critical organ (case 2); iii) a patient with liver tumor, and iv) a patient with prostate cancer. The patient data were obtained from the CORT dataset (Craft et al 2014). The treatment plans differed with respect to tumor site, target volume, location of OARs, total dose, number of fractions, and beam field configuration. For all plans, the longitudinal and lateral spot spacing was set to 3 mm. For the RBE calculation, all VOIs were assigned an α/β ratio of 2 Gy for photon irradiation. The methodology can naturally be extended to different α/β ratios being assigned to different VOIs should this information be available. A summary of the treatment plans, along with the plan optimization settings for the reference plans (RBE-weighted dose optimization only), is shown in Table 1.

For case 1 of the water phantom, the reference plan was designed to deliver 60 Gy (RBE) to the PTV using two orthogonal (AP-LR) fields. For the evaluation of simultaneous optimization, the reference plan was modified to include an objective to enhance the number of large ionization clusters in a sub-region centered in the PTV representing a radioresistant compartment of the tumor. Different values for the penalty of the objective on ID were evaluated with penalty values ranging from 0 to 40. For the case of ID objective penalty equal to zero, the simultaneously optimized plan is equivalent to the reference plan.

For case 2 of the water phantom, an OAR representing a critical organ near the tumor, overlapping with the PTV, was placed at the distal end of the LR field. In the plans accounting for simultaneous optimization, an objective function was included to reduce the number of large ionization clusters in this OAR. The penalty of the objective on ID in the critical organ was evaluated in the range from 0 to 0.24 and the value of 0.24 was chosen to demonstrate the results of simultaneous optimization. This scenario is analogous to the goal to minimize the LET in the brainstem present in the PTV, e.g., (Unkelbach et al 2016), replacing LET with the number of large ionization clusters.

The liver tumor was planned with two fields at gantry angles 240° and 300° and couch angle 0° (RPO-RAO fields). The simultaneously optimized plan was obtained to achieve a higher degree of homogeneity of the number of large ionization clusters in the voxels comprising the PTV, i.e., by means of minimizing the variance of the number of large ionization clusters in the VOI. This goal can be considered equivalent to increasing the homogeneity of the radiation quality across the target volume to achieve a uniform tumor response. The penalties $p_{\nu L}$ for the objective on ID ranged from 0 (reference plan) to 10000 (maximally weighted ID-optimized plan).

The prostate cancer was irradiated with two opposing LR-RL fields. In this case, a simultaneous optimization plan was designed to reduce the number of large ionization clusters in the rectum. Because this could also be achieved with an objective to reduce the dose in the rectum, an alternative to the reference plan was also generated where an objective function penalizing dose in the rectum was included. The penalties $p_{\nu L}$ in the rectum ranged from 0 to 20.

In order to evaluate the impact of the relative penalties $p_{\nu L}/p_d$, for the number of large ionization clusters and RBE-weighted dose, respectively, a quality indicator, QI_X, to measure the level of inhomogeneity of the distribution of a quantity X across a volume-of-interest was defined as follows:

$$QI_X = \frac{|\, Q_X(95\,\%) - Q_X(5\,\%)\,|}{Q_X(50\,\%)}$$

where $QI_X(N\%)$ corresponds to the N% quantile of the distribution of X. In all results of simultaneous optimization presented below, $p_{\nu L}$ was chosen in such a way that QI_{RBExD} in the PTV was not substantially impaired by the inclusion of extra objectives on the number of large ionization clusters. Furthermore, the impact of the simultaneous optimization on the plan quality was constrained in order that all treatment plans satisfy the following conditions: target dose coverage in the PTV was evaluated for all plans to ensure that 95% of the volume is covered by 95% of the reference dose and the maximum dose is below 107% of the reference dose.

3 Results

3.1 Large ionization clusters can be enhanced in the target for equivalent RBE-weighted dose

We first demonstrate simultaneous optimization of RBE-weighted dose and ionization clustering for the simple geometry of the water phantom, case 1, with a centered PTV and a sub-region in the PTV where the radiation quality was modified by increasing the frequency of large ionization clusters. In the simultaneous optimization, an objective was added to enhance the number of large ionization clusters in the sub-region representing the situation of a more radioresistant compartment of the tumor.

Figure 1 presents the dependence of the mean number of large ionization clusters in the PTV sub-region and the inhomogeneity index of the RBE-weighted dose in the PTV on the relative penalty $p_{\nu L}/p_d$ for the objectives on the number of large ionization clusters and RBE-weighted dose. When increasing the penalty $p_{\nu L}$ from 0 to 40 for a fixed value of p_d equal to 800, the mean number of large ionization clusters in the PTV sub-region increased by 7.3% from 179.5 to 192.6 10^6/μg. At the same time, the higher priority for the objective on the number of large ionization clusters affects the target dose conformity with the increase in the inhomogeneity index for the RBE-weighted dose in the PTV from 0.005 for the reference plan to 0.066 for the simultaneous optimization with $p_{\nu L}$ equals to 40 ($p_{\nu L}/p_d$ of 0.05). Other quality indicators are also affected by the simultaneous optimization. D_{max}

increases by 5.8% from 60.31 to 63.82 Gy (RBE) while D_{95} decreases by 1.7% from 59.87 to 58.86 Gy (RBE).

Figure 2 presents the central axial slice through the target volume showing the distributions of the number of large ionization clusters for the reference plan and the plan that enhances the number of large ionization clusters in the central sub-region of the PTV corresponding to $p_{vL}/p_d = 40/800 = 0.05$. The number of large ionization clusters achieved with the simultaneous optimization strategy was increased in the whole PTV sub-region. Minor changes of the radiation quality were also observed in the remaining volume of the PTV and outside the PTV, while no substantial effect was observed on the RBE-weighted dose distribution (results not shown).

The results of the validation of the treatment plan obtained with the simultaneous optimization for the cubic water phantom, case 1, irradiated by orthogonal carbon beams are shown in figure 3. It includes the γ-analysis for the physical dose, RBE-weighted dose and large ionization clusters in the central axial plane. A pass rate of 99.3%, 98.5% and 100% was observed for the physical dose, RBE-weighted and the density of large ionization clusters, respectively.

3.2 Large ionization clusters in a critical organ overlapping the PTV can be reduced

The simple geometry of the water box phantom, case 2 with a critical organ partially overlapping the PTV was used to evaluate how the radiation quality can be optimized to spare OARs located in the treatment field. The simultaneous optimization included an objective to reduce the number of large ionization clusters in the region of overlap between the PTV and the critical organ.

Figure 4 presents the central axial slice through the target volume showing the distributions of the number of large ionization clusters for the reference plan and the plan that reduces the number of large ionization clusters. A selective reduction of the number of large ionization clusters in the region of the critical organ located in the PTV can be obtained with the simultaneous optimization with the inhomogeneity index of the RBE-weighted dose in the PTV increasing from 0.002 to 0.051. With the simultaneous optimization, the D_{95} in the PTV was reduced from 59.97 to 57.36 Gy (RBE), while the mean number of large clusters in the overlapping region between the critical organ and PTV decreased from 180.3 to 159.3 $10^6/\mu g$ (i.e., 11.6% decrease).

The results of the validation of the treatment plan obtained with the simultaneous optimization for the cubic water phantom, case 2, irradiated by orthogonal carbon beams are shown in figure 5. It includes the γ-analysis for the physical dose, RBE-weighted dose and large ionization clusters in the central axial plane. A pass rate of 99.1%, 98.3% and 99.9% was observed for the physical dose, RBE-weighted and the density of large ionization clusters, respectively.

3.3 Higher uniformity of radiation quality in the tumor volume is possible with simultaneous optimization

The liver tumor plan was used to evaluate the possibility of improving the homogeneity of the radiation quality across the tumor volume with simultaneous optimization. To this end, an objective to minimize the variance of the number of large ionization clusters was added. The quality indicators for the target dose conformity and the number of large ionization clusters were calculated as a function of the relative penalties $p_{\nu L}/p_d$ in the range of 0 to 20 for $p_d = 500$.

Table 2 shows the quality indicators of dose, D_{max}, D_{mean}, D_5, and D_{95}, as well as the 5%, 50% and 95% quantiles for the number of large ionization clusters, $\nu_L(5)$, $\nu_L(50)$, $\nu_L(95)$, for five plans with increasing ratios for the penalties on the number of large ionization clusters and dose ($p_{\nu L}/p_d$) in the PTV. No meaningful effect of the increase in the relative penalties was observed for the mean RBE-weighted dose in the PTV, but it led to a monotonic decrease in D_{95} from 44.62 Gy (RBE) for the reference plan (i.e., $p_{\nu L}/p_d$ equals to zero) to 43.67 Gy (RBE) for the highest relative penalty of $p_{\nu L}/p_d = 20$. On the other hand, a more pronounced increase in $\nu_L(5)$ and a more pronounced decrease in $\nu_L(95)$ is observed. The variation of QI for the RBE-weighted dose and the number of large ionization clusters as a function of the relative penalties $p_{\nu L}/p_d$ are shown in Figure 6.

Figure 6 shows a substantial reduction of the inhomogeneity of the number of large ionization clusters in the PTV with increasing $p_{\nu L}/p_d$. This is mirrored by a relatively lower loss of the target dose conformity. The results with simultaneous optimization for a relative penalty of 10 was chosen to visualize the impact on the distributions of RBE-weighted dose and number of large ionization clusters.

Figures 7 and 8 show the distributions of RBE-weighted dose and the absolute number of large ionization clusters, respectively. In order to minimize the variance of the number of large ionization clusters in the PTV, the optimizer increases the number of large ionization clusters in the proximal region of the SOBP by increasing the intensity of pencil beams stopping in this region. However, this also led to an increase in dose and the number of large ionization clusters in the healthy tissues located in the beam path, as no competing constraints/objectives were set to restrict such an effect in the entry region. An increase in dose in the region where the heart bordered the PTV was also observed, but the dose there was below the constraint of 25 Gy (RBE) set for the reference plan (Table 2).

Figure 9 shows the volume histograms of RBE-weighted dose, large ionization clusters, and dose-averaged LET in the PTV, heart and skin for the reference plan and the plan obtained with the simultaneous optimization of dose and number of large ionization clusters in the PTV. An improved uniformity of the distribution of large ionization clusters in the PTV is obtained using the simultaneous optimization approach while the impact on the target dose conformity is small. As large ionization clusters are mainly produced by high-LET radiation, the optimization of the number of large ionization clusters also affects the LET distribution in the target. The higher uniformity of the distribution of large ionization clusters in the PTV also leads to higher uniformity of the LET distribution. The results indicate that the

simultaneous optimization presents a comparable dose distribution in the target with a considerable change in the radiation quality in its volume.

3.4 The number of large ionization clusters in OARs can be minimized in two ways to reduce complications

As the absolute number of large ionization clusters scales with dose, it is possible to indirectly reduce the number of large ionization clusters in an OAR by simply adding an objective to penalize dose in the VOI. To evaluate how this approach compares to simultaneous optimization, the reference plan for the prostate cancer was modified to include an extra objective for the rectum to either i) penalize any dose (p_d of 50 with a reference value of 0) or ii) penalize large ionization clusters (p_{vL} of 2 or 20).

The quality indicators for dose and number of large ionization clusters in the rectum are presented in Table 3. The mean dose in the rectum for all plans was well below the maximum tolerance dose of 50 Gy (RBE) set in the optimization settings for the reference plan (Table 1). Nonetheless, there was substantial room for further reduction of the dose in this OAR as demonstrated by the results of the modified reference plan and the plans with simultaneous optimization. As for the number of large ionization clusters, a substantial reduction of the mean and the 50% quantile was observed for the plans with the extra objectives to reduce either dose or the number of large ionization clusters in the rectum. As for the dose in the PTV, the extra objectives led to an increase in the spread of the RBE-weighted dose distribution. The plans with simultaneous optimization showed a comparable degradation of the dose in the PTV as the modified reference plan with the extra objective to reduce dose in the rectum. The three plans lead to substantial reduction of the mean dose and number of large clusters in the rectum in comparison to the reference plan.

The results of simultaneous optimization and the plan with reduction of dose in the rectum showed a similar decrease in the number of large ionization clusters in the rectum for equivalent dose distribution in the PTV. Thus, the number of large ionization clusters can be optimized in treatment planning to spare OARs and reduce the risks of normal tissue complication.

4 Discussion

The simultaneous optimization of RBE-weighted dose and ionization details in nanometric volumes was investigated for the first time using existing IMPT planning tools in carbon-ion therapy. In simultaneous optimization, the number of large ionization clusters (more than 3 ionizations) in nanometric volumes was used as a surrogate for radiation quality and additional objectives of this parameter were added to the objectives related to RBE-weighted dose. Thereby, one can realize an alternative optimization procedure of radiation effect without foregoing the current procedure of optimization based on RBE-weighted dose. This should be a safer approach than giving up an already established optimization concept for one that has not yet been used in clinical practice nor experimentally. The first results indicate that a simultaneous optimization of dose and large ionization clusters is, in fact, possible, allowing the optimization of both RBE-weighted dose and ionization clustering end-points in target and OAR.

While in carbon ion therapy the optimization of effective dose has relied on RBE modeling, there is a large uncertainty in RBE estimation (Karger and Peschke 2018). Different RBE models which have been considered for clinical application show variation in their prediction of RBE for tumor response and normal tissue complications (e.g., Gillmann et al 2014, Gillmann et al 2018, Saager et al 2015). An accurate RBE model for all endpoints of interest would suffice for treatment plan optimization. However, as such a solution is yet to be provided, we expect that carbon ion therapy could profit from the optimization of radiation quality based on ID. Besides, the uncertainty in RBE modeling is, among other factors, a function of radiation quality. Since a reduction of the variability of radiation quality could be related to a more homogeneous biological effect, the simultaneous optimization approach could be applied to reduce the impact of the uncertainties of RBE.

It was shown that the results of the optimization for combined objective functions based on dose and ionization clustering are sensitive to the relative penalties for the different quantities. In particular, the choice of the penalty values for the objectives based on dose and ionization clustering allows the definition of a custom trade-off between radiation quality within a specific VOI while controlling the cost on the target dose conformity. This is particularly true for the weighted sum of objectives and it could be overcome by prioritized optimization as in Unkelbach et al (2016).

As observed for the water phantom in case 1, large ionization clusters can be enhanced in a sub-region of the target volume for equivalent RBE-weighted dose distribution otherwise. Such a scheme could be applied to potentially increase the induction of complex DNA damage in more radioresistant/hypoxic compartments of a tumor to overcome the resistance to radiation. The nanometric ID optimization approach is particularly appealing if the radiation field is composed of different types of charged particles with different fluences and LET values. Nonetheless, it should be recognized that redistribution of ID within regions of interest also implies a redistribution of ID outside of the regions of interest, which may violate normal tissue dose constraints. A more specific evaluation of the overall therapeutic gain of simultaneous optimization of RBE-weighted dose and ID is beyond the scope of this initial work, because it will require radiobiological experiments and analysis of human data in carefully designed clinical trials.

For case 2 of the water phantom, it was shown that simultaneous optimization can be used to spare an OAR overlapping with the PTV from receiving a relatively high number of large ionization clusters, which may increase the number of late effects. Such a situation could be of interest, for example, to reduce complex DNA damages in critical structures which cannot be spared of high dose due to their proximity to the tumor volume. In this way, additional objectives to optimize the radiation quality may help to reduce the probability of complications in critical structures.

While the uniform RBE-weighted dose distribution in the target volume is designed to yield uniform radiobiological effect in the tumor, our results indicate that radiobiological models based on LET alone may have non-uniform ID, which could result in variation in cell killing across a homogeneous tumor. In this case, simultaneous optimization of RBE-weighted dose uniformity and radiation quality uniformity during treatment planning could be applied to

achieve a higher uniformity of the tumor response. The results of the investigation of the liver tumor indicate that a higher uniformity of radiation quality in the tumor volume can be achieved in intensity-modulated carbon-ion therapy at a moderate loss in target dose conformity. In particular, in this investigation, the simultaneous optimization allowed for a substantial reduction of the variance of the distribution of large ionization clusters in the target volume. Assuming that the cell response to large clustered DNA damages is less sensitive to the cell conditions (e.g., cell cycle, oxygen level) and that large ionization clusters are an appropriate surrogate for large clustered DNA damage, a more uniform distribution of RBE-weighted dose combined with uniformity of large ionization clusters in the tumor could reduce the variability of the cell response, although this remains to be experimentally verified.

In an optimal IMPT plan scenario, the biologically effective dose delivered to OARs should be kept to a minimum. However, due to the difficulties in predicting the occurrence of normal tissue complications, it is desirable to avoid irradiating such structures with a radiation quality indicating high effectiveness of inducing clustered damages to the DNA. Because it is reasonable to expect a correlation of clustered DNA damage with large ionization clusters, simultaneous optimization could be applied to reduce the number of large ionization clusters and RBE-weighted dose in OARs.

Tumor control probability (TCP) is typically characterized by a steep slope on the dose response curve which can translate into high sensitivity of local control to dose inhomogeneities in the tumor. Therefore, it is important to emphasize that the impact of simultaneous optimization should be evaluated in light of changes in TCP, which was beyond the scope of the present investigation.

The presented methodology for the calculation of the density of large ionization clusters makes use of the pencil beam algorithm which has limitations for the dose calculations in the case of heterogeneous structures. The same limitations are expected for the calculation of large ionization clusters. Therefore, in the case of heterogeneities, Monte Carlo simulations using the condensed-history method can be used to calculate the distributions of dose and large ionization clusters required for the treatment plan optimization. Considering the recent developments of fast Monte Carlo engines for carbon-ion beams (Qin et al 2018), the future of carbon-ion radiotherapy is likely to make use of the Monte Carlo method in treatment planning, providing accurate calculations of radiation quality in the patient. Then, simultaneous optimization could produce an optimal distribution of radiation quality in the patient that maximizes tumor control and minimizes normal tissue complications.

In this study, large ionization cluster size was used as a surrogate of radiation quality, being closely tied to biological effect but independent of conventional RBE modeling. Alternative choices of ID may also be conducive to simultaneous optimization while possibly providing a better match to biological effect. This work focused on carbon-ion therapy, while the approach is applicable to protons and other ions. Because clustered ionizations in nanometric volumes are expected to correlate with biological effectiveness and risk for late effects, simultaneous optimization could also provide a larger therapeutic benefit.

5 Conclusions

We describe a novel IMPT planning strategy that enables the simultaneous optimization of RBE-weighted dose and nanometric ionization clustering in carbon-ion therapy. The results indicate that radiation quality-related nanodosimetric end-points in the target volume and OARs can be simultaneously accounted for in the optimization procedure without impairing the RBE-weighted dose distribution obtained with current practice. Because the distributions are affected both inside and outside the target volume, the optimization should take into account both tumor control and normal tissue complication probabilities to obtain a good therapeutic ratio. This has yet to be accomplished for the ID as an identifier of radiation quality and proven to be possible with radiobiological and clinical data. When sufficient radiobiological and clinical evidence has accumulated, this strategy could be applied to achieve better tumor control and reduce risks of complications with the ultimate goal of improving the clinical outcome.

References

Agostinelli S et al. 2003 GEANT4 – a simulation toolkit Nucl. Instrum. Methods A 506 250–303

Allison J et al. 2006 Geant4 developments and applications IEEE Trans. Nucl. Sci 53 270–8

Bassler N, Jäkel O, Søndergaard CS and Petersen JB 2010 Dose- and LET-painting with particle therapy Acta Oncol. 49 1170–76 doi: 10.3109/0284186X.2010.510640 [PubMed: 20831510]

Cao W, Khabazian A, Yepes PP, Lim G, Poenisch F, Grosshans DR and Mohan R 2018 Linear energy transfer incorporated intensity modulated proton therapy optimization Phys. Med. Biol 63 015013 doi: 10.1088/1361-6560/aa9a2e

Casiraghi M and Schulte RW 2015 Nanodosimetry-Based Plan Optimization for Particle Therapy Comp Math Methods in Medicine 2015 908971 doi: 10.1155/2015/908971

Conte V, Selva A, Colautti P, Hilgers G and Rabus H 2017 Track structure characterization and its link to radiobiology *Radiat.* Meas. 106 506–11 doi: 10.1016/j.radmeas.2017.06.010

Craft D, Bangert M, Long T, Papp D and Unkelbach J 2014 Shared data for intensity modulated radiation therapy (IMRT) optimization research: the CORT dataset GigaScience 3

Garty G, Schulte R, Shchemelinin S, Leloup C, Assaf G, Breskin A, Chechik R, Bashkirov V, Milligan J and Grosswendt B 2010 A nanodosimetric model of radiation-induced clustered DNA damage yields Phys. Med. Biol 55 761–82 doi: 10.1088/0031-9155/55/3/015 [PubMed: 20071772]

Elsässer T and Scholz M 2007 Cluster effects within the local effect model Radiat. Res 167 319–29 [PubMed: 17316069]

Giantsoudi D, Grassberger C, Craft D, Niemierko A, Trofimov A and Paganetti H 2013 Linear Energy Transfer-Guided Optimization in Intensity Modulated Proton Therapy: Feasibility Study and Clinical Potential Int. J. Radiat. Oncol. Biol. Phys 87 216–22 doi: 10.1016/j.ijrobp.2013.05.013 [PubMed: 23790771]

Gillmann C, Jäkel O, Schlampp I, Karger CP 2014 Temporal lobe reactions after carbon ion radiation therapy: comparison of relative biological effectiveness-weighted tolerance doses predicted by local effect models I and IV Int. J. Radiat. Oncol. Biol. Phys 88 1136–41 [PubMed: 24661667]

Gillmann C, Lomax AJ, Weber DC, Jäkel O, Karger CP 2018 Dose–response curves for MRI-detected radiation-induced temporal lobe reactions in patients after proton and carbon ion therapy: Does the same RBE-weighted dose lead to the same biological effect? Radiother. Oncol 128 109–14 [PubMed: 29459152]

Granville D A, Sawakuchi G O 2015 Comparison of linear energy transfer scoring techniques in Monte Carlo simulations of proton beams Phys. Med. Biol 60 N283–N291 [PubMed: 26147442]

Grosswendt B, Pszona A and Bantsar A 2007 New descriptors of radiation quality based on nanodosimetry, a first approach Radiat. Prot. Dosim 126 432–44

Hawkins RB 2003 A microdosimetric-kinetic model for the effect of non-Poisson distribution of lethal lesions on the variation of RBE with LET Radiat. Res 160 61–9 [PubMed: 12816524]

Inaniwa T, Furukawa T, Kase Y, Matsufuji N, Toshito T, Matsumoto Y, Furusawa Y and Noda K 2010 Treatment planning for a scanned carbon beam with a modified microdosimetric kinetic model Phys. Med. Biol 55 6721–37 [PubMed: 21030747]

Inaniwa T, Kanematsu N, Noda K, Kamada T 2017 Treatment planning of intensity modulated composite particle therapy with dose and linear energy transfer optimization Phys. Med. Biol 62 5180–97 [PubMed: 28333688]

Jäkel O, Krämer M, Karger C and Debus J 2001 Treatment planning for heavy ion radiotherapy: clinical implementation and application Phys. Med. Biol 46 1101–16 [PubMed: 11324954]

Karger CP and Peschke P 2018 RBE and related modeling in carbon-ion therapy Phys. Med. Biol 63 01TR02

Krämer M and Scholz M 2000 Treatment planning for heavy ion radiotherapy: calculation and optimization of biologically effective dose Phys. Med. Biol 45 3319–30 [PubMed: 11098906]

Lindborg L and Nikjoo H 2011 Microdosimetry and radiation quality determinations in radiation protection and radiation therapy Radiat. Prot. Dosim 143 402–8

Low D, Harms W, Mutic S, Purdy JA 1998 A technique for the quantitative evaluation of dose distributions Med Phys. 25 656–61. [PubMed: 9608475]

Paganetti H 2014 Relative biological effectiveness (RBE) values for proton beam therapy. Variations as a function of biological endpoint, dose, and linear energy transfer Phys. Med. Biol 59 R419–72 [PubMed: 25361443]

Parodi K, Mairani A and Sommerer F 2013 Monte Carlo-based parametrization of the lateral dose spread for clinical treatment planning of scanned proton and carbon ion beams J. Radiat. Res 54 i91–6 doi: 10.1093/jrr/rrt05, doi: 10.1093/jrr/rrt05 [PubMed: 23824133]

Perl J, Shin J, Schumann J, Faddegon B and Paganetti H 2012 TOPAS: an innovative proton Monte Carlo platform for research and clinical applications Med. Phys 39 6818–37 doi: 10.1118/1.4758060 [PubMed: 23127075]

Rabus H and Nettelbeck H 2011 Nanodosimetry: Bridging the gap to radiation biophysics Radiat. Meas 46 1522–8.

Ramos-Méndez J, Burigo LN, Schulte R, Chuang C and Faddegon B 2018 Fast calculation of nanodosimetric quantities in treatment planning of proton and light-ion therapy (Accepted)

Rossi HH and Zaider M 1991 Elements of microdosimetry Med. Phys 18 1085–92 [PubMed: 1753890]

Qin N, Shen C, Tsai MY, Pinto M, Tian Z, Dedes G, Pompos A, Jiang SB, Parodi K and Jia X 2018 Full Monte Carlo–Based Biologic Treatment Plan Optimization System for Intensity Modulated Carbon Ion Therapy on Graphics Processing Unit Int. J. Radiat. Oncol. Biol. Phys 100 235–43 doi: 10.1016/j.ijrobp.2017.09.002 [PubMed: 29079118]

Saager M, Glowa C, Peschke P, Brons S, Grün R, Scholz M, Huber PE, Debus J, Karger CP 2015 Split dose carbon ion irradiation of the rat spinal cord: Dependence of the relative biological effectiveness on dose and linear energy transfer Radiother. Oncol 117 358–63 [PubMed: 26197953]

Scholz M and Kraft G 1996 Track structure and the calculation of biological effects of heavy charged particles Adv. Space Res 18 5–14

Scholz M, Kellerer AM, Kraft-Weyrather W and Kraft G 1997 Computation of cell survival in heavy ion beams for therapy. The model and its approximation Radiat. Environ. Biophys 36 59–66 [PubMed: 9128899]

Tinganelli W, Durante M, Hirayama R, Krämer M, Maier A, Kraft-Weyrather W, Furusawa Y, Friedrich T and Scifoni E 2015 Kill-painting of hypoxic tumours in charged particle therapy Sci. Rep 5 17016 doi: 10.1038/srep17016

Unkelbach J, Botas P, Giantsoudi D, Gorissen BL and Paganetti H 2016 Reoptimization of Intensity Modulated Proton Therapy Plans Based on Linear Energy Transfer Int. J. Radiat. Oncol. Biol. Phys 96 1097–106 doi: 10.1016/j.ijrobp.2016.08.038 [PubMed: 27869082]

Wieser HP, Cisternas E, Wahl N, Ulrich S, Stadler A, Mescher H, Müller LR, Klinge T, Gabrys H, Burigo L, Mairani A, Ecker S, Ackermann B, Ellerbrock M, Parodi K, Jäkel O and Bangert M

2017 Development of the open-source dose calculation and optimization toolkit matRad Med. Phys 44 2556–68 doi: 10.1002/mp.12251 [PubMed: 28370020]

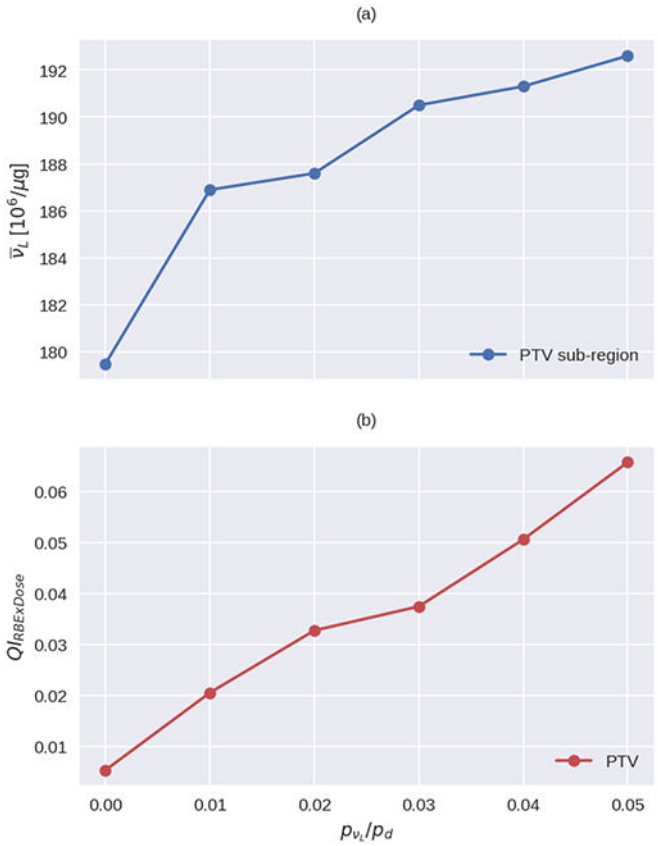

Figure 1 –.

Effect of the relative penalties $p_{\nu L}/p_d$ for the objectives on (a) the mean number of large ionization clusters in the PTV sub-region, and (b) the inhomogeneity index of RBE-weighted dose on the PTV.

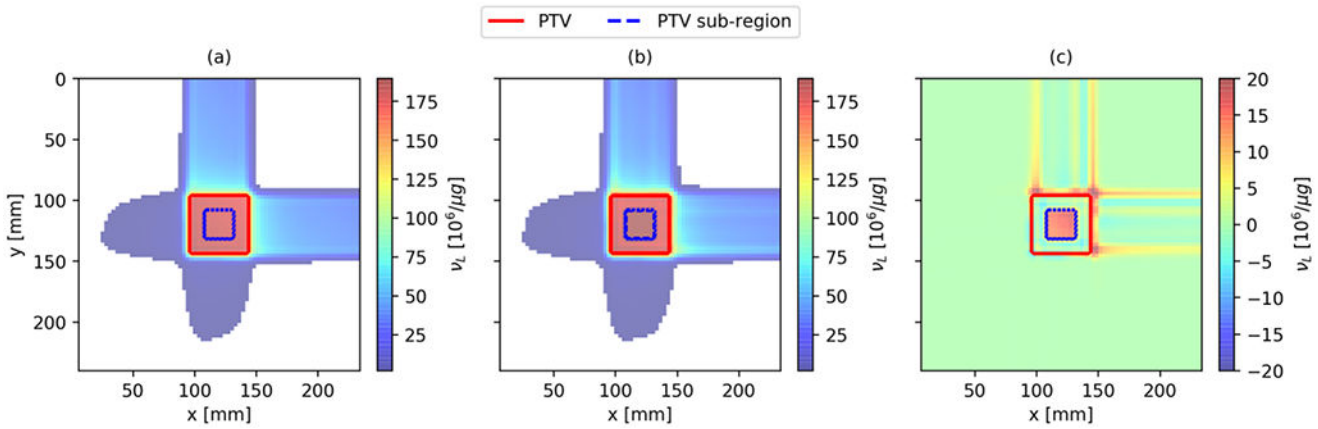

Figure 2 –.

The cubic water phantom, case 1, irradiated by orthogonal carbon beams: The distribution of large ionization clusters is shown in the central axial plane for (a) the reference plan, (b) the plan with simultaneous optimization; (c) shows the difference maps between these plans. The plan with simultaneous optimization was designed to enhance the number of large ionization clusters in the PTV sub-region centered in the PTV using $p_{\nu L}$= 40. Positive values (red) indicate a greater number of large ionization clusters in the plan obtained with simultaneous optimization.

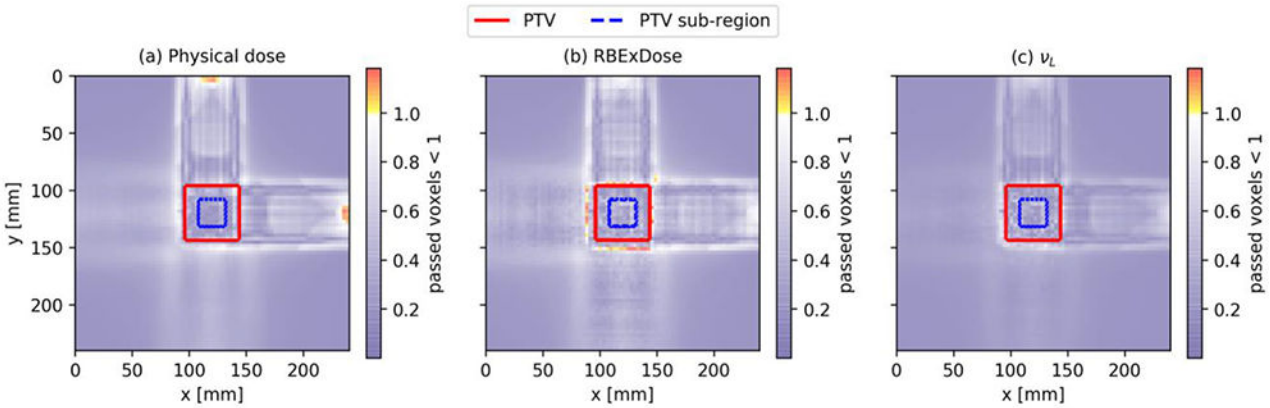

Figure 3 –.

Validation of the simultaneous optimization for the cubic water phantom, case 1, irradiated by orthogonal carbon beams using $p_{\nu L}$= 40: γ-analysis evaluation for results from matRad against Monte Carlos simulations using 2 mm/2% pass criterion for (a) physical dose, (b) RBE-weighted dose, (c) large ionization clusters.

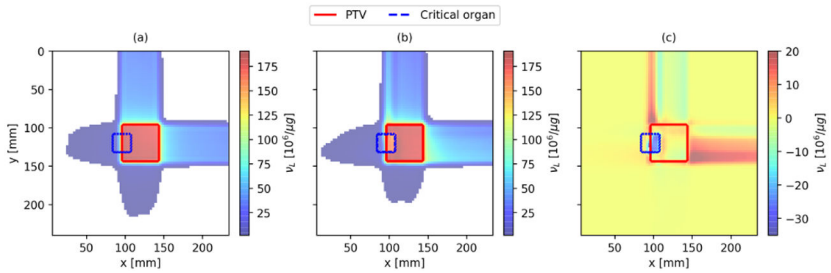

Figure 4 –.

Distribution of the number of large ionization clusters in (a) the reference plan, and (b) the simultaneous optimization, as well as (c) the difference of the number of large ionization clusters in the two plans in axial plane for the case 2 of the water phantom. The plan with simultaneous optimization was designed to minimize the number of large ionization clusters in the region of overlap between the PTV and the critical organ.

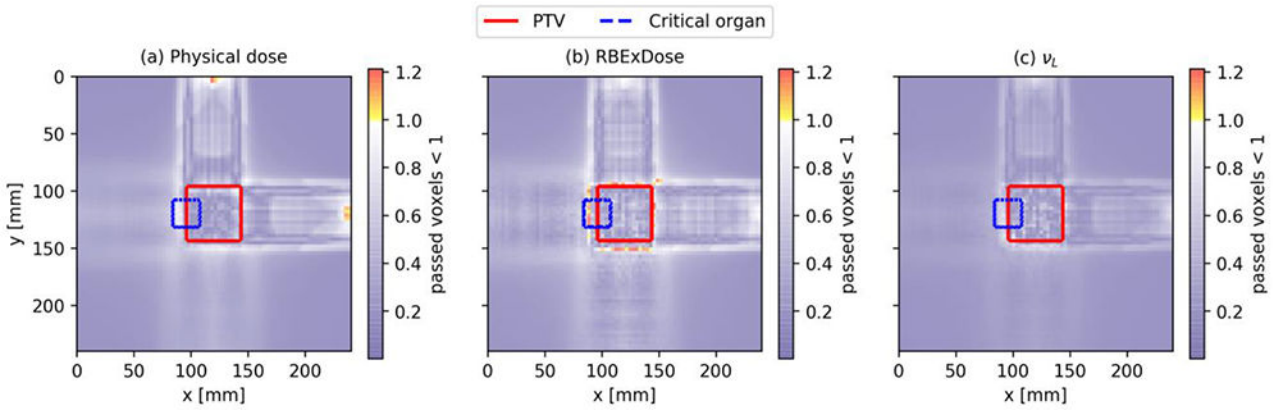

Figure 5 –.

Validation of the simultaneous optimization for the cubic water phantom, case 2, irradiated by orthogonal carbon beams using $p_{\nu L}$= 0.24: γ-analysis evaluation for results from matRad against Monte Carlos simulations using 2 mm/2% pass criterion for (a) physical dose, (b) RBE-weighted dose, (c) large ionization clusters.

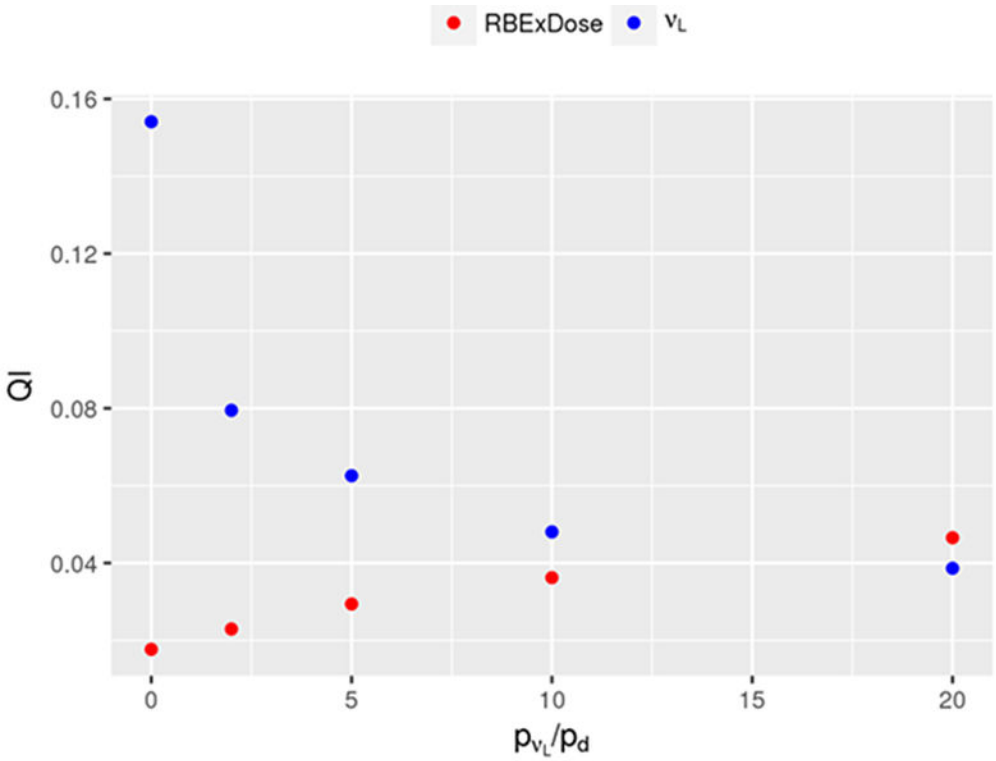

Figure 6 –.

Index of inhomogeneity of the RBE-weighted dose and the number of large ionization clusters in the PTV for the liver tumor case as a function of relative penalties for the number of large ionization clusters and dose.

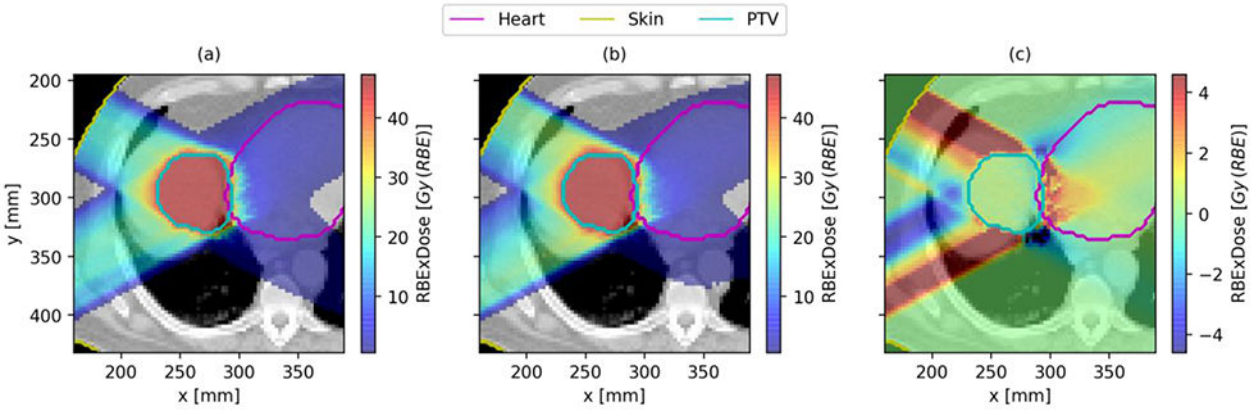

Figure 7 –.

Distribution of RBE-weighted dose in the central axial plane of the liver tumor obtained with different optimization strategies: (a) reference plan, (b) simultaneous optimization plan; (c) difference of RBE-weighted dose in the two plans. The plan with simultaneous optimization was designed to reduce the variance of the number of large ionization clusters in the PTV with penalty ratio of $p_{\nu L}/p_d = 10$.

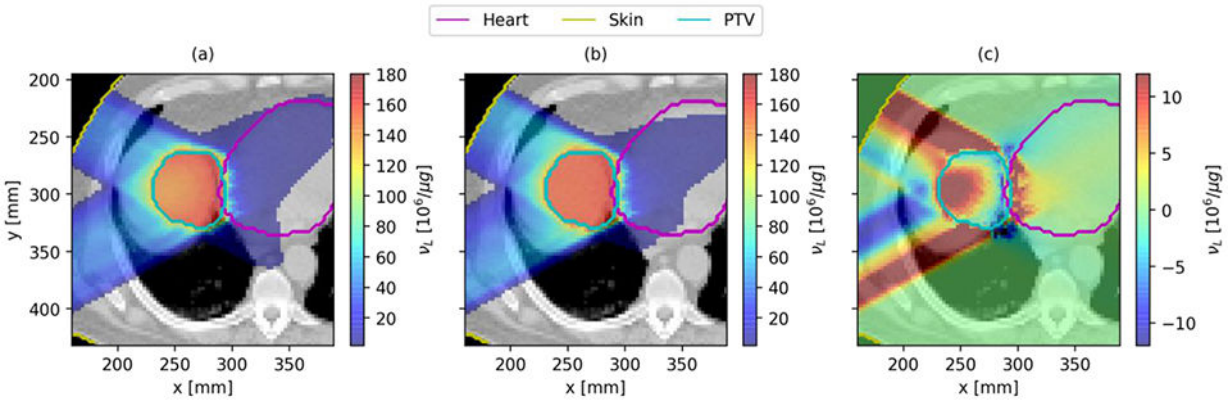

Figure 8 –.

Distribution of the number of large ionization clusters in the central axial plane of the liver tumor: (a) reference plan, (b) simultaneous optimization plan; (c) difference of large ionization clusters in the two plans. The plan with simultaneous optimization was designed to reduce the variance of the number of large ionization clusters in the PTV with $p_{\nu L}/p_d$ of 10.

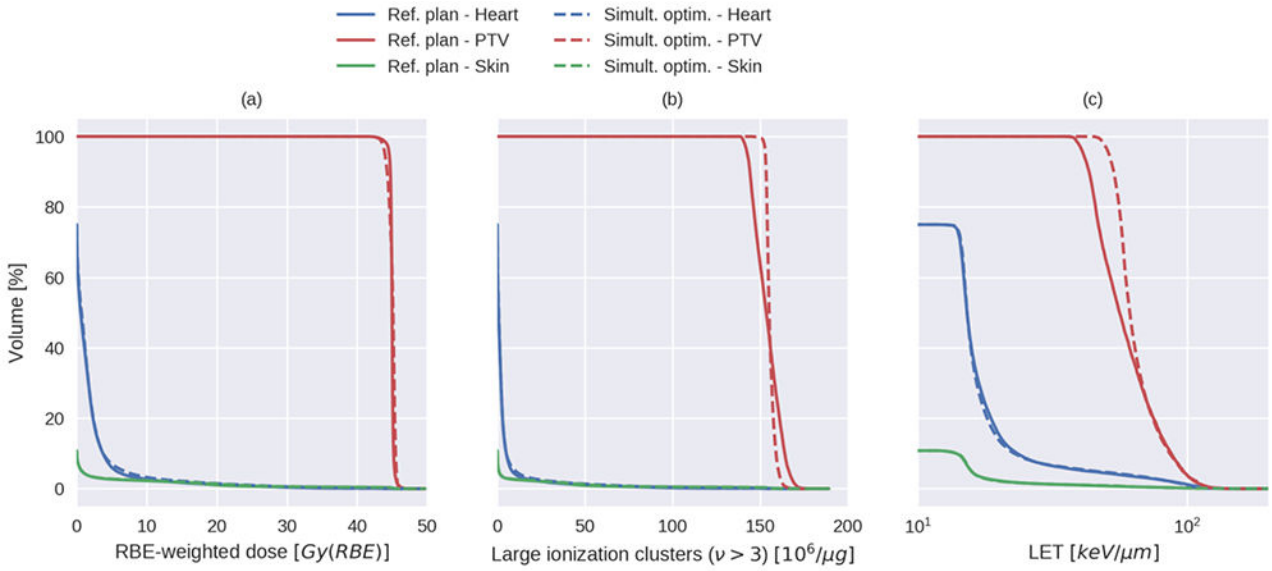

Figure 9 –.

Volume histograms in the PTV, and heart and skin of a) RBE-weighted dose, b) large ionization clusters, and c) dose-average LET, for the reference and simultaneous optimization plans for the liver tumor. Results of the simultaneous optimization plan were obtained with an additional objective to minimize the variance of large ionization clusters in the PTV using a relative penalty p_{vL}/p_d of 10.

Table 1 –

Treatment plan parameters including geometry (phantom, tumor site), field configurations (A-anterior, P-posterior, L-left, R-right, O-oblique), number of fractions (FX), VOI considered in the plan optimization, VOI type (target or OAR), VOI volume, RBE-weighted reference dose, optimization criteria and penalty for the reference IMPT plan.

Site (Field configurations)	FX	VOI	VOI type	VOI volume [cm^3]	Reference plan optimization		
					Dose objective	Dose [Gy (RBE)]	Penalty
Water phantom, case 1 (AP-LR)	20	PTV	Target	110.6	Squared deviation	60	800
		Radioresistant region	Target	13.8	Squared deviation	60	800
		Surrounding	OAR	105.4	Squared overdosing	45	100
Water phantom, case 2 (AP-LR)	20	PTV	Target	110.6	Squared deviation	60	800
		Critical organ	OAR	13.8	Squared overdosing	60	800
		Surrounding	OAR	105.4	Squared overdosing	45	100
Liver (RPO-RAO)	10	PTV	Target	156.5	Squared deviation	45	500
		Heart	OAR	743.0	Squared overdosing	25	300
		Skin	OAR	43365.5	Squared overdosing	25	300
Prostate (LR-RL)	20	PTV68 *(1)*	Target	182.8	Squared deviation	68	1000
		PTV68 *(1)*	Target	182.8	Max dose constraint	72.8	1000
		PTV56 *(2)*	Target	256.3	Squared deviation	56	1000
		Pelvis	OAR	18640.1	Squared overdosing	30	100
		Bladder	OAR	313.1	Squared overdosing	50	300
		Rectum	OAR	47.6	Squared overdosing	50	200

(1) Region of PTV with planned reference dose of 68 Gy (RBE)

(2) Region of PTV with planned reference dose of 56 Gy (RBE)

Table 2 –

Quality indicators of RBE-weighted dose, D_{max}, D_{mean}, D_5, $D_{50,}$ and D_{95}, and number of large ionization clusters, represented by the 5%, 50% and 95% quantiles $\nu_L(5)$, $\nu_L(50)$, $\nu_L(95)$, for five plans with different ratios for the penalties on the objective based on the number of large ionization clusters and dose ($p_{\nu L}/p_d$) from 0 to 20 in the PTV. The relative penalty of zero corresponds to the liver tumor reference plan in Table 1.

$p_{\nu L}/p_d$	D_{max} [Gy (RBE)]	D_{mean} [Gy (RBE)]	D_5 [Gy (RBE)]	D_{95} [Gy (RBE)]	$\nu_L(5)$ [10^6/μg]	$\nu_L(50)$ [10^6/μg]	$\nu_L(95)$ [10^6/μg]
0	47.35	45.00	45.41	44.62	142.8	153.5	166.4
2	46.84	44.99	45.37	44.33	150.9	154.2	163.2
5	46.61	45.00	45.48	44.15	152.1	154.8	161.8
10	46.41	45.02	45.61	43.98	153.1	155.2	160.6
20	46.45	44.99	45.77	43.67	153.3	155.0	159.3

Table 3 –

Quality indicators of dose, D_{mean}, $D_{5,}$ and D_{10}, and number of large ionization clusters, represented by the mean, 50% and 95% quantiles $\nu_{L,mean}$, $\nu_L(50)$, $\nu_L(95)$ in the rectum, and the inhomogeneity index of RBE-weighted dose in the PTV receiving 68 Gy (RBE).

Plan	D_{mean} [Gy (RBE)]	D_5 [Gy (RBE)]	D_{10} [Gy (RBE)]	$\nu_{L,\,mean}$ [10^6/μg]	$\nu_L(50)$ [10^6/μg]	$\nu_L(95)$ [10^6/μg]	$QI_{RBExDose}$
Reference plan	22.69	65.66	50.45	53.56	43.53	195.1	0.0342
Modified reference plan	12.50	57.04	33.72	26.77	11.17	158.3	0.0484
Simultaneous optimization ($p_{\nu L}$ = 2)	14.07	62.78	40.76	30.35	13.02	181.4	0.0416
Simultaneous optimization ($p_{\nu L}$ = 20)	11.92	51.15	28.67	24.06	11.25	131.8	0.0574